Peptides 37 (2012) 273–284

Contents lists available at SciVerse ScienceDirect

Peptides

journal homepage: www.elsevier.com/locate/peptides

Protein transduction in human cells is enhanced by cell-penetrating peptides fused with an endosomolytic HA2 sequence

Ji-Sing Liou[a,b], Betty Revon Liu[a,b], Adam L. Martin[c], Yue-Wern Huang[d,*], Huey-Jenn Chiang[b], Han-Jung Lee[a,**]

[a] Department of Natural Resources and Environmental Studies, National Dong Hwa University, No. 1, Sec. 2, Da-Hsueh Road, Shoufeng, Hualien 97401, Taiwan
[b] Graduate Institute of Biotechnology, National Dong Hwa University, No. 1, Sec. 2, Da-Hsueh Road, Shoufeng, Hualien 97401, Taiwan
[c] Department of Biological Sciences and the cDNA Resources Center, Missouri University of Science and Technology, 206 Schrenk Hall, 400 West 11th Street, Rolla, MO 65409-1120, USA
[d] Department of Biological Sciences, Missouri University of Science and Technology, 105 Schrenk Hall, 400 West 11th Street, Rolla, MO 65409-1120, USA

ARTICLE INFO

Article history:
Received 15 June 2012
Received in revised form 21 July 2012
Accepted 23 July 2012
Available online 31 July 2012

Keywords:
Cell-penetrating peptide
Cytotoxicity
Endosomal escape
Hemagglutinin-2
Membrane fusion

ABSTRACT

Endocytosis has been proposed as one of the primary mechanisms for cellular entry of cell-penetrating peptides (CPPs) and their cargoes. However, a major limitation of endocytic pathway is entrapment of the CPP-cargo in intracellular vesicles from which the cargo must escape into the cytoplasm to exert its biological activity. Here we demonstrate that a CPP tagged with an endosomolytic fusion peptide derived from the influenza virus hemagglutinin-2 (HA2) remarkably enhances the cytosolic delivery of proteins in human A549 cells. To determine the endosome-disruptive effects, recombinant DNA plasmids containing coding sequences of HA2, CPPs and red fluorescent proteins (*RFPs*) were constructed. The fusion proteins were purified from plasmid-transformed *Escherichia coli*, and their effects on protein transduction were examined using live cell imaging and flow cytometry. Our data indicate that endocytosis is the major route for cellular internalization of CPP-HA2-tagged RFP. Mechanistic studies revealed that the fusogenic HA2 peptide dramatically facilitates CPP-mediated protein entry through the release of endocytosed RFPs from endosomes into the cytoplasm. Furthermore, incorporating the HA2 fusion peptide of the CPP-HA2 fusion protein improved cytosolic uptake without causing cytotoxicity. These findings strongly suggest that the CPP-HA2 tag could be an efficient and safe carrier that overcomes endosomal entrapment of delivered therapeutic drugs.

1. Introduction

While many small molecules, such as ions, sugars and amino acids, permeate cells through carriers and channels in the plasma membrane, this mode of entry is generally unavailable for macromolecules, such as proteins, DNAs and RNAs. In order to develop highly efficient strategies for the controlled cellular delivery of bioactive macromolecules with therapeutic potential, several non-viral carrier systems, including liposomes, polycationic carriers, nanomaterials and peptides, have been developed. Cell-penetrating peptides (CPPs), also called protein transduction domains (PTDs), are a group of short, highly basic peptides that are able to penetrate the cell membrane either alone or carried with cargoes [9]. In 1988, two groups independently discovered that the transactivator of transcription (TAT) protein of the human immunodeficiency virus type 1 (HIV-1) can penetrate cells and activate viral genome replication [16,21]. The process by which TAT protein and other CPPs cross the cell membrane and deliver macromolecule cargoes is referred to as protein transduction [11,31,50]. CPPs can be categorized into three groups based upon their composition [35]. The first group is comprised of protein-derived peptides, such as PTD of TAT and antennapedia. The second group includes chimeric peptides, such as transportan, that contain two or more motifs from different peptides [41]. The last group is comprised of synthetic peptides, such as polyarginines [17].

Although protein transduction has been widely used as a research tool, and twenty clinical trials are now testing

Abbreviations: BFP, blue fluorescent protein; CPP, cell-penetrating peptide; CytD, cytochalasin D; EEA1, early endosome antigen 1 protein; GFP, green fluorescent protein; FITC, fluorescein isothiocyanate; HA, hemagglutinin; HA2, hemagglutinin-2; MTT, 1-(4,5-dimethylthiazol-2-yl)-3,5-diphenylformazan; 6His, hexa-histidine; NLS, nuclear localization signal; PBS, phosphate buffered saline; PTD, protein transduction domain; QD, quantum dot; R9, nona-arginine; RFP, red fluorescent protein; SUMO, small ubiquitin-related modifier; TAT, transactivator of transcription.

* Corresponding author. Tel.: +1 573 341 6589; fax: +1 573 341 4821.
** Corresponding author. Tel.: +886 3 8633642; fax: +886 3 8633260.
E-mail addresses: huangy@mst.edu (Y.-W. Huang), hjlee@mail.ndhu.edu.tw (H.-J. Lee).

0196-9781/$ – see front matter © 2012 Elsevier Inc. All rights reserved.
http://dx.doi.org/10.1016/j.peptides.2012.07.019

CPP-mediated delivery of drug conjugates in patients with a variety of diseases [48], the mechanisms of CPP-mediated cellular uptake and the subsequent intracellular trafficking are still under extensive investigation. Presently, it is believed that most CPPs utilize multiple pathways for cellular entry [35,37,43,48]. The two major uptake mechanisms of CPPs are direct membrane translocation and endocytosis. Direct membrane translocation, also called direct cell penetration, encompasses a variety of energy-independent pathways, including pore formation, inverted micelle formation, carpet-like model and membrane thinning model [35,48]. Endocytosis is divided into two major categories; phagocytosis involves the uptake of large particles while pinocytosis involves solute uptake [23,35]. Pinocytosis can be further divided into macropinocytosis, clathrin-dependent, caveolin-dependent and clathrin/caveolin-independent pathways [6]. Numerous factors, including the experimental conditions and physicochemical properties of CPPs and their cargoes, appear to influence the route of cellular uptake [35,48].

Insofar as endocytosis is one of the primary mechanisms for cellular delivery mediated by CPPs, the fate of endocytosed cargoes is of paramount importance. Endocytosed cargoes often become trapped in organelles, such as vesicles, endosomes, lysosomes and macropinosomes [42], where they may be degraded by hydrolytic enzymes. Thus, escape from endocytic vesicles into the cytoplasm is essential to preserve biological activity of endocytosed cargoes and becomes a limiting factor in the usage of CPPs to deliver bioactive molecules [11,35,43,48,51]. Recently, several endosome-disruptive peptides (membrane destabilizing/fusion peptides) were derived from certain pathogens, including viruses and bacterial toxins [37]. These membrane-disrupting peptides are triggered by endosomal acidification and promote endosomal escape [12,39,51].

The human influenza virus is an enveloped virus that contains two major envelope glycoproteins, hemagglutinin (HA) and neuraminidase [58]. HA is composed of two subunits: hemagglutinin-1 responsible for binding to cells and hemagglutinin-2 (HA2) responsible for endosomal escape. The N-terminal domain of the HA2 subunit possesses 23 amino acids (GLFGAIAGFIENGWEGMIDGWYG), a relatively hydrophobic region referred to as fusion peptide [7,56]. This fusion peptide domain is buried in the HA trimer in its resting conformation. Acidification in the endosome triggers an irreversible conformational change of HA2, exposing the fusion peptide and allowing it to insert itself into endosomal membranes. Subsequent formation of a fusion pore results in membrane fusion and leading to transfer of viral genome into the cytosol [7]. The INF7 (GLFEAIEGFIENGWEGMIDGWYG) peptide, a glutamic acid-enriched HA2 analog, was identified as a more potent endosome membrane-destabilizing peptide [40]. In this peptide, two glutamic acid moieties (underlined in peptide sequence) were introduced into the original HA2 fusion peptide to extend the α-helix structure, thereby increasing pH sensitivity [14]. HA2 was used to enhance CPP-mediated endosomal escape of cargoes [13,18,28–30,36,45,46,51,61,62].

Certain delivered molecules are intended to target nucleus. Molecules can enter the nucleus from the cytoplasm by both passive diffusion and active transport mechanisms [10]. Small molecules less than 10 nm in diameter or 50–60 kDa in size can diffuse through nuclear pore complexes [50]. Most protein molecules are transported by energy-dependent transport mechanisms mediated by nuclear localization signals (NLS). These signals are recognized by importin family proteins that mediate the transport across the nuclear envelope with the participation of Ran-GTP [10].

The goals in the present study were to (1) compare the transduction efficiency of CPP-, HA2- and/or NLS-tagged red fluorescent proteins (RFPs) and (2) determine the uptake mechanisms and subcellular localization of these proteins. To achieve these goals, we first constructed a series of novel DNA plasmids containing coding sequences of CPP, HA2 and/or NLS fused *RFP*. These plasmids were expressed in bacteria, and the transduction efficiency of these fusion proteins was determined in human lung cancer A549 cells using live cell imaging and flow cytometry. To elucidate the uptake mechanisms, pharmacological and physical inhibitors were used to block cellular uptake processes. We found that uptake of CPP-HA2-tagged RFP involves energy-dependent endocytosis. This study with constructed CPP-containing plasmids reveals valuable mechanistic insights into how these CPPs cause endosomal escape and provides a basis for the design of optimized delivery agents.

Table 1
Sequences of tags.

Tag	Amino acid sequence (single letter code)
HA2 (INF7)	GLFEAIEGFIENGWEGMIDGWYG
6His	HHHHHH
NLS	PKKKRKV
R9	RRRRRRRRR

2. Materials and methods

2.1. Plasmid construction

The mCherry plasmid (kindly provided by Dr. Roger Y. Tsien, University of California, San Diego, CA, USA) is a prokaryotic expression vector that encodes a hexa-histidine (6His)-tagged monomeric *RFP* sequence (Table 1) [44]. The pR9-mCherry plasmid containing a nona-arginine (R9, a CPP) and HA tag (YPYDVPDYA) fused *RFP* coding region under the control of the T7 promoter was described previously [54]. This HA tag does not appear to interfere with the bioactivity of recombinant fusion proteins and facilitates the detection, isolation and purification of many protein fusions [47]. The pR9-HA2-mCherry plasmid consisting of an R9 and HA2 (INF7) fused *RFP* coding sequence was constructed by the annealing and digestion of two overlapping primers (HA2-U [5′-TTAGATCTAGGCCTATTCGAGGCAATAGAAGGTTTCATAGAAAATGGTTGGGA-3′, with the *Bgl*II site underlined] and HA2-D [5′-TTGGATCCCCGTACCAACCGTCTATCATTCCCTCCCAACCATTTTCTATGAAA-3′, with the *Bam*HI site underlined]) cloned into the *Bam*HI site of the pR9-mCherry plasmid. The pR9-NLS-mCherry plasmid containing an R9 and NLS fused *RFP* was generated using two overlapping 5′ phosphorylated primers (NLS-U [5′-GATCCCAAGAAGAAGAGGAAAGTC-3′] and NLS-D [5′-GATCGACTTTCCTCTTCTTCTTGG-3′]) cloned into the *Bam*HI site of the pR9-mCherry plasmid. The pR9-HA2-NLS-mCherry plasmid consisting of an R9, HA2 and NLS fused *RFP* was constructed by cloning the NLS-U/D fragment at the *Bam*HI site of the pR9-HA2-mCherry plasmid. All constructs were confirmed by DNA sequencing.

2.2. Protein purification and characterization

Protein expression and purification were as described previously with modifications [3,27]. All plasmid constructs were transformed into *Escherichia coli* KRX strain (Promega, Madison, WI, USA). Bacteria were grown to OD_{600} = 0.4 and then induced with 0.1% (w/v) rhamnose (Sigma-Aldrich, St. Louis, MO, USA) overnight at 37 °C. Expressed proteins were purified by metal chelation chromatography. The binding (5 mM imidazole, 0.5 M NaCl, 20 mM Tris–HCl, pH 7.9) and wash (80 mM imidazole, 0.5 M NaCl, 20 mM Tris–HCl, pH 7.9) buffers were used during purification. Purified proteins were concentrated as well as dialyzed using Amicon Ultra-4 centrifugal filter devices (Millipore, Billerica, MA, USA) and quantified by a protein assay kit (Bio-Rad, Hercule, CA, USA).

Luminescent images of proteins were captured using the Typhoon FLA 9000 Biomolecular Imager (GE Healthcare, Piscataway, NJ, USA) with the excitation wavelength at 532 nm for RFPs [32]. Emission spectra of RFPs were evaluated using an EnSpire 2300 Multilabel Reader (PerkinElmer, Waltham, MA, USA) with excitation at 488 nm and emission varying from 510 to 700 nm.

2.3. Protein transduction, subcellular colocalization and mechanistic assays

Human lung carcinoma A549 cells (American Type Culture Collection, Manassas, VA, USA; CCL-185) were cultured in Roswell Park Memorial Institute (RPMI) 1640 medium (Gibco, Invitrogen, Carlsbad, CA, USA) containing phenol red supplemented with 10% (v/v) bovine serum (Gibco), as previously described [54]. To determine the optimal concentration for protein transduction, cells were seeded at a density of 1×10^5 cells per 35-mm petri dish and then incubated overnight in 1 ml of growth medium. Cells were washed twice with 1 ml of phosphate buffered saline (PBS) and then treated with various proteins at the final concentrations of 1, 5, 10, 30 and 60 μM in RPMI 1640 medium with neither phenol red nor serum at 37 °C for 1 h. Cells were washed five times with PBS to remove free proteins.

To determine subcellular colocalization, cells were treated with 30 μM of various proteins for different durations (30 min, 1, 3, 6, 12, 18 and 24 h) in RPMI medium with neither phenol red nor serum at 37 °C. Cells were washed with PBS for five times to remove free proteins followed by staining with fluorescent organelle-specific trackers [27]. Hoechst 33342, LysoSensor Green DND-153 (Invitrogen) and fluorescein isothiocyanate (FITC) mouse anti-human early endosome antigen 1 protein (EEA1) antibody (BD Biosciences, Franklin Lakes, NJ, USA) were utilized to visualize nuclei, lysosomes and early endosomes, respectively. Fluorescent images were detected using a BD Pathway 435 System (BD Biosciences).

To conduct energy-dependent uptake experiments, cells were incubated for 30 min at 4 °C at which temperature energy-dependent molecular movement in the cell membrane is essentially arrested [49]. Cells were then treated with 30 μM of R9-HA2-mCherry at 4 °C for 6 h followed by staining with Hoechst 33342 for 40 min and LysoSensor trackers for 30 min. The influence of modulators that inhibit or enhance uptake processes was studied in cells treated without or with cytochalasin D (CytD), nocodazole [33] or chloroquine (Sigma–Aldrich) [60]. Cells were pretreated in the absence or presence of 10 μM of CytD, 10 μM of nocodazole or 25 μM of chloroquine at 37 °C for 30 min. These cells were then treated with 30 μM of R9-HA2-mCherry in the absence or presence of CytD or nocodazole at 37 °C for 6 h, or chloroquine for 12 h followed by staining with Hoechst 33342 and LysoSensor trackers. To test any synergistic effect of the HA2 and chloroquine combination [57], cells were pretreated in the absence or presence of chloroquine at 37 °C for 30 min. These cells were then treated with 30 μM of R9-mCherry or R9-HA2-mCherry in the absence or presence of chloroquine for 12 h.

To assess the CPP-HA2-mediated cargo delivery, cells were treated with collagen-fluorescein (Sigma–Aldrich) [23], R9-HA2-mCherry or R9-HA2-mCherry/collagen-fluorescein complexes at various ratios. Fluorescent images were detected using a BD Pathway 435 System (BD Biosciences).

2.4. Confocal and fluorescent microscopy

Fluorescent and bright-field live cell images were recorded using a BD Pathway 435 System (BD Biosciences) equipped with the Olympus 20× and 60× oil objectives (Olympus, Tokyo, Japan) [27]. This system includes both confocal and fluorescent microscopy sets. Excitation filters were set at 377/50 nm, 482/35 nm and 543/22 nm for blue, green and red fluorescence, respectively. Emission filters were set at 435LP (long-pass), 536/40 nm and 593/40 nm for blue (BFP), green fluorescent protein (GFP) and RFP channels, respectively. Transmitted light with the 536/40 nm emission filter was used to observe cell morphology as bright-field images.

2.5. Flow cytometric analysis

A549 cells were seeded at a density of 1×10^5 cells per well in 24-well plates and then incubated overnight in 500 μl/well of culture medium. Cells were treated with five proteins for designated durations (1, 5, 10, 30, 60 min, 3, 6, 12, 18 and 24 h) in RPMI medium with neither phenol red nor serum at 37 °C and then washed five times with PBS. Cells were analyzed using a Cytomics FC500 Flow Cytometer (Beckman Coulter, Fullerton, CA, USA), as previously described [24]. For RFP detection, excitation was set at 488 nm and emission at 615 nm with a FL3 filter. Results are reported as the percentage of the total cell population.

2.6. Cytotoxicity assay

A549 cells were plated at a density of 1×10^4 cells in 96-well plates and incubated overnight in 200 μl/well of growth medium. Cells were treated with 1, 5, 10, 30 and 60 μM of five proteins in RPMI medium without phenol red nor serum, washed with PBS, and cultured in RPMI medium without serum at 37 °C for 24 h. Cells were treated with PBS as a negative control and 70% alcohol as a positive control. Cytotoxicity was assessed by the ability of the cells to reduce 1-(4,5-dimethylthiazol-2-yl)-3,5-diphenylformazan (MTT) [23,54]. MTT absorbance was measured at 570 nm wavelength using a Model 680 Microplate Reader (Bio-Rad).

2.7. Statistical analysis

Data are expressed as mean ± standard deviation. Mean values and standard deviations were calculated from at least three independent experiments carried out in triplicates in each group. Statistical comparisons between the control and treated groups were performed by the Student *t*-test, using levels of statistical significance of $P < 0.05$ (*, †, ‡) and 0.01 (**, ††, ‡‡), as indicated.

3. Results

3.1. RFP-fusion protein analysis

To examine the endosomolytic effect of HA2, we constructed several CPP-containing RFP expression plasmids (Fig. 1). The mCherry, R9-mCherry, R9-HA2-mCherry, R9-NLS-mCherry, and R9-HA2-NLS-mCherry proteins were overexpressed and purified in *E. coli* KRX strain transformed with the relevant plasmids. These plasmids produced 6His-tagged RFP alone or in-frame fused RFPs with a combination of R9, HA2 and NLS (Table 1) under the control of the T7 promoter. SDS-PAGE analysis of purified mCherry, R9-mCherry, R9-HA2-mCherry, R9-NLS-mCherry and R9-HA2-NLS-mCherry fusion proteins was detected by a luminescent imager (Fig. 2A) or by staining with Coomassie brilliant blue (Fig. 2B). The five purified recombinant RFPs have calculated molecular masses of 30.6–36.4 kDa. Luminescent scan revealed emission spectra of the fluorescent RFPs (Fig. 3). All RFPs had maximal emission at about 610 nm upon excitation at 488 nm, indicating that the fluorescent property of the RFP-fusion proteins is not compromised by the addition of peptide tags to the original RFP.

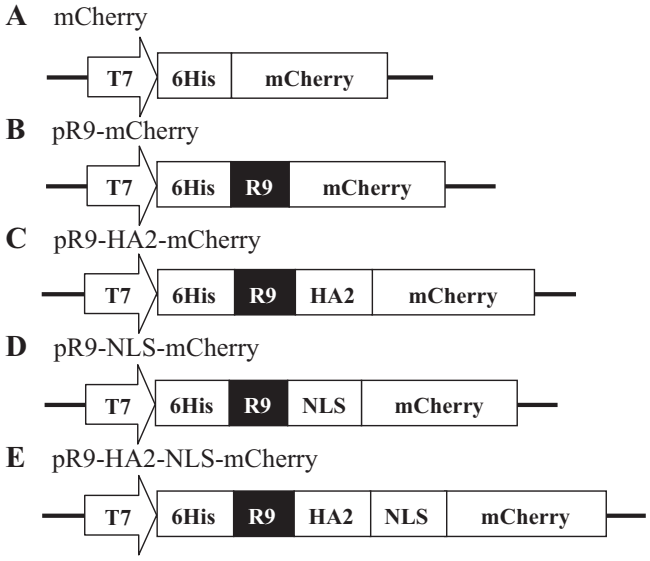

Fig. 1. Schematic structure of DNA plasmids. (A) The mCherry plasmid. This is the original bacterial expression cassette containing the coding region of a hexahistidine (6His)-tagged monomeric *RFP* under the control of the T7 promoter. (B) The pR9-mCherry plasmid. This plasmid contains a nona-arginine (R9) tagged *RFP* coding sequence. (C) The pR9-HA2-mCherry plasmid. This plasmid contains an R9 and HA2 (INF7) tagged *RFP* coding sequence. (D) The pR9-NLS-mCherry plasmid. This plasmid contains an R9 and nuclear localization signal (NLS) tagged *RFP* coding sequence. (E) The pR9-HA2-NLS-mCherry plasmid. This plasmid contains an R9, HA2 and NLS tagged *RFP* coding sequence.

3.2. Protein transduction efficiency of RFPs

To determine the optimal concentration for protein transduction, human A549 cells were treated with various concentrations of mCherry, R9-mCherry or R9-HA2-mCherry proteins for 1 h. No fluorescent signal was detected by flow cytometric analysis in the cells treated with mCherry (Fig. 4). Red fluorescent signal was observed in the cells treated with R9-mCherry at the concentration of 60 μM, which is consistent with our previous results [2,24,34,54]. Remarkably, the cells treated with ≥1 μM of R9-HA2-mCherry exhibited significantly higher fluorescence intensity than those treated with equivalent concentrations of mCherry or R9-mCherry. The intensity of the fluorescent signal in R9-HA2-mCherry treated cells was concentration-dependent. Measurements of protein transduction were obtained by confocal imaging. A549 cells were treated with a series of concentrations of mCherry (Fig. 5A), R9-mCherry (Fig. 5B) or R9-HA2-mCherry (Fig. 5C) proteins for 30 min, stained with Hoechst 33342 and then imaged. The imaging data were in good accordance with the above results of flow cytometric analysis, confirming that HA2 tag is able to remarkably increase CPP-mediated protein transduction activity. After 30 min, R9-HA2-mCherry was primarily located around the inner perimembraneous area. According to Figures 4 and 5, 30 μM of fluorescent proteins were chosen as the optimal concentration for subsequent experiments due to more clear and consistent images.

3.3. Time course analysis of CPP-HA2-mediated protein transduction

To understand the kinetics of protein transduction, cells were treated with mCherry, R9-mCherry, R9-HA2-mCherry, R9-NLS-mCherry or R9-HA2-NLS-mCherry fluorescent proteins, and cellular uptake of proteins was measured at various time points by flow cytometry. The cells treated with R9-HA2-mCherry at 5 min showed higher red fluorescent intensity than the cells treated with the other four proteins (Fig. 6A). The fraction of the

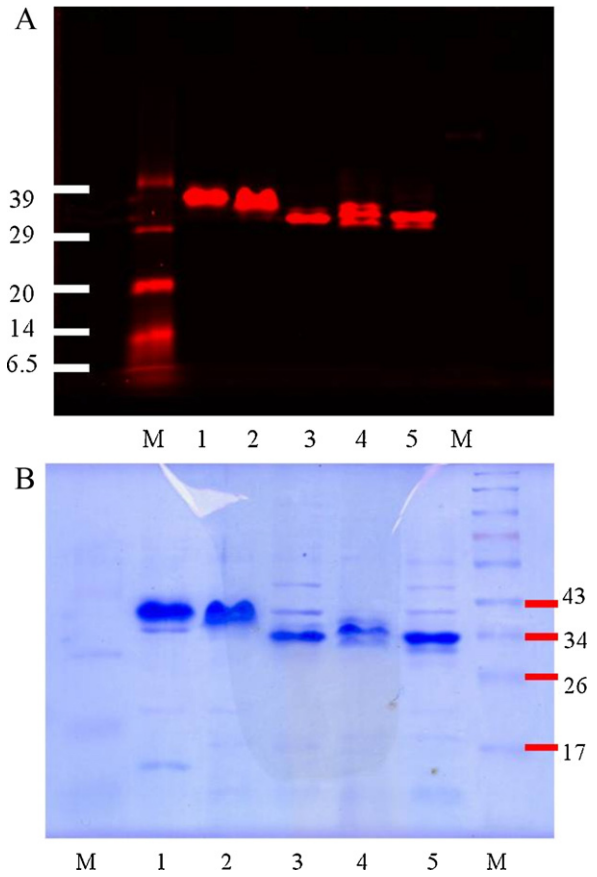

Fig. 2. SDS-PAGE analysis. (A) Luminescent photography. (B) Coomassie brilliant blue stain. Purified mCherry, R9-mCherry, R9-HA2-mCherry, R9-NLS-mCherry and R9-HA2-NLS-mCherry proteins are in lanes 1–5, respectively. Red fluorescent (F3401, Fluorescent Low Molecular Weight Markers, Sigma) and standard protein markers (SM0671, Fermentas, Glen Bumie, MD, USA) are displayed on the left and right lanes M, respectively. (For interpretation of the references to color in this figure legend, the reader is referred to the web version of the article.)

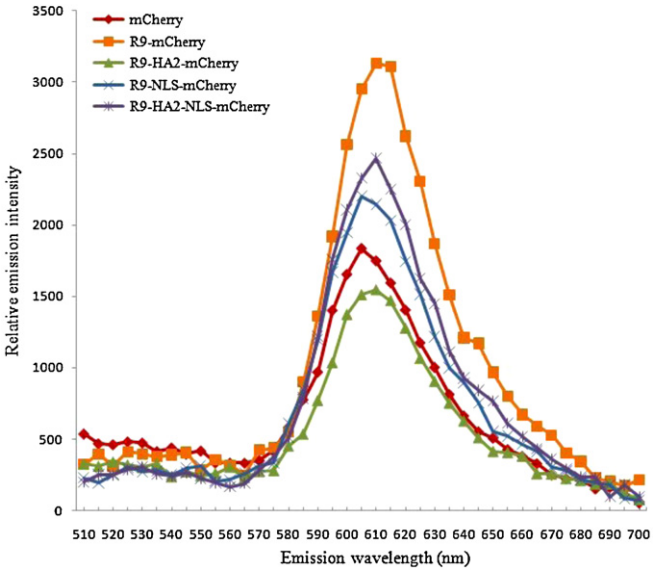

Fig. 3. Luminescent emission spectra of RFPs. Five purified mCherry, R9-mCherry, R9-HA2-mCherry, R9-NLS-mCherry and R9-HA2-NLS-mCherry proteins were evaluated by divergent emission scan for their optical absorption using an EnSpire 2300 Multilabel Reader (PerkinElmer).

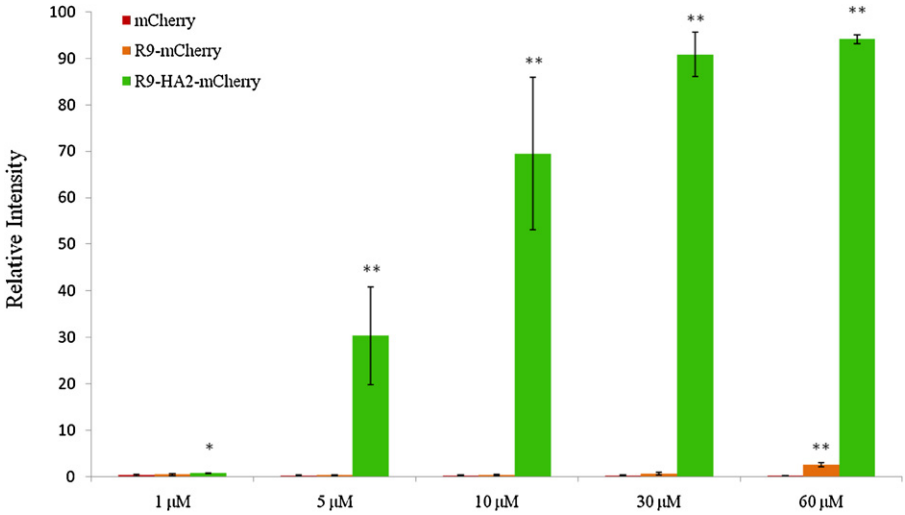

Fig. 4. Flow cytometric analysis of protein transduction by RFPs. A549 cells were treated with 1, 5, 10, 30 and 60 μM of mCherry, R9-mCherry or R9-HA2-mCherry for 1 h and analyzed using a Cytomics FC500 flow cytometer (Beckman Coulter). Data are presented as mean ± standard deviation from three independent experiments. Significant differences were determined at $P < 0.05$ (*) and $P < 0.01$ (**).

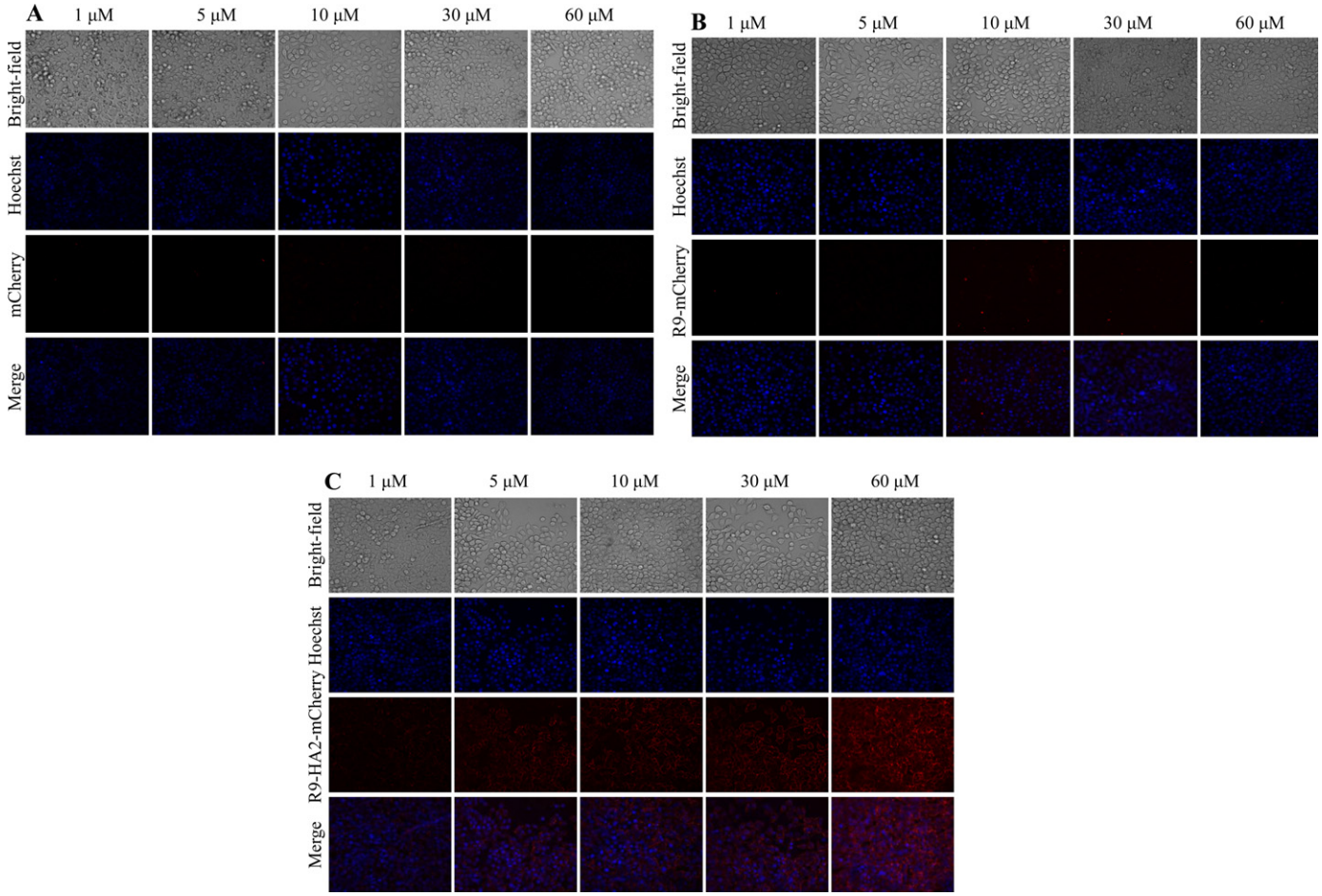

Fig. 5. Confocal microscopy of protein transduction of RFPs. Cells were treated with 1, 5, 10, 30 and 60 μM of mCherry (A), R9-mCherry (B) or R9-HA2-mCherry (C) for 30 min and stained with Hoechst 33342. Images were recorded using a BD pathway system at a magnification of 200×. RFP and BFP channels in the microscope are used to reveal the distribution of fluorescent proteins and nuclei, respectively. Overlap between fluorescent proteins and nuclei exhibits purple color in merged RFP and BFP images.

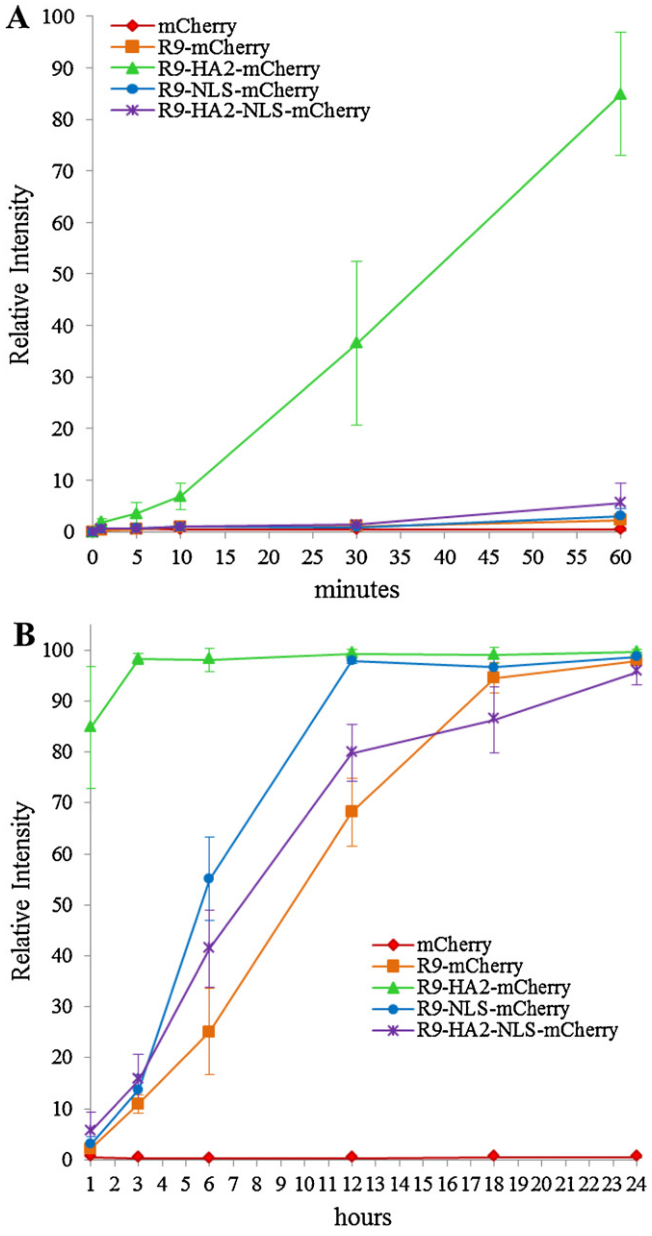

Fig. 6. Time course analysis of CPP-HA2-mediated protein transduction. Cells were treated with 30 μM of mCherry, R9-mCherry, R9-HA2-mCherry, R9-NLS-mCherry or R9-HA2-NLS-mCherry for short (1, 5, 10, 30 and 60 min) (A) and long (1, 3, 6, 12, 18 and 24 h) (B) periods of time and then analyzed by a flow cytometer. Data are presented as mean ± standard deviation from three independent experiments.

R9-HA2-mCherry treated cells with fluorescence continued to increase over time. At 1 h, the R9-HA2-mCherry group showed 80 times higher protein uptake than the other groups. When the time point was extended to 18 h, the uptake of R9-mCherry, R9-HA2-mCherry, R9-NLS-mCherry and R9-HA2-NLS-mCherry fluorescent proteins reached about 90% of all cells (Fig. 6B). These results confirm that HA2 peptide accelerates endosomolytic activity to increase CPP-mediated protein transduction. Moreover, NLS tags seemed to inhibit HA2 enhancement of protein transduction.

To study the endosomolytic ability of HA2, cells were treated with mCherry, R9-mCherry, R9-HA2-mCherry, R9-NLS-mCherry or R9-HA2-NLS-mCherry proteins for 1, 3, 6, 12, 18 and 24 h, stained with organelle-specific green fluorescent markers and then analyzed by confocal microscopy. No red fluorescence could be detected in the cells treated with mCherry at any time (Fig. 7A). In contrast, the cells treated with R9-mCherry (Fig. 7B) and R9-NLS-mCherry (data not shown) proteins exhibited a time-dependent increase in red fluorescence in the cytoplasm, a few yellow/orangey spots in lysosomes but not the nuclei. Strikingly, the cells treated with R9-HA2-mCherry displayed red fluorescence in plasma membrane at 1 h, around the inner perimembraneous area at 3 h and throughout the cytosol after 6 h (Fig. 7C). Results from the cells treated with R9-HA2-NLS-mCherry (data not shown) were similar to those of R9-HA2-mCherry treatment, although the uptake was lower. Further, we noticed some yellow/orangey punctate formations within the cells treated with R9-HA2-mCherry after 6 h (Fig. 7C and D) and R9-HA2-NLS-mCherry after 12 h (Fig. 7D), suggesting that these proteins were associated with lysosomes and endosomes. Together, these results suggest that the pathway of cellular internalization of R9-HA2-mCherry and R9-HA2-NLSmCherry involves endocytosis. The fusogenic HA2 peptide dramatically enhanced CPP-mediated protein transduction apparently by helping the escape of RFPs from endosomes into the cytoplasm.

3.4. Energy-dependent mechanism of CPP-HA2-mediated protein transduction

To reveal the mechanistic aspect of R9-HA2-mCherry internalization, cells were treated with R9-HA2-mCherry at 4 °C or 37 °C (as a control) for 6 h (Fig. 8A). Low temperature incubation inhibited cellular uptake of R9-HA2-mCherry (Fig. 8A and B). These data are in agreement with the results in Fig. 7C and suggest that protein transduction of R9-HA2-mCherry involves energy-dependent endocytosis.

To examine the molecular aspect of endocytic processes, cells were treated with R9-mCherry or R9-HA2-mCherry in the absence or presence of CytD, nocodazole or chloroquine. Both endocytic inhibitors, CytD and nocodazole, disrupted cellular uptake of R9-HA2-mCherry (Fig. 8B). The lysosomotropic agent chloroquine further enhanced the cellular uptake of R9-HA2-mCherry compared to that of R9-mCherry (Fig. 8C and D). However, the combination of chloroquine and HA2 fusion peptide did not produce a synergistic increase of protein transduction (Fig. 8D).

3.5. MTT-based cell viability assay

To assess cytotoxicity caused by CPPs tagged with HA2 and/or NLS in eukaryotes, A549 cells were treated with mCherry, R9-mCherry, R9-HA2-mCherry, R9-NLS-mCherry or R9-HA2-NLS-mCherry proteins for 24 h and then analyzed by the MTT reduction assay (Fig. 9). Cells treated with PBS and 70% alcohol were used as negative and positive controls, respectively. Cells treated with 1, 5, 10, 30 and 60 μM of any of RFP-fusion proteins did not display cytotoxicity.

3.6. CPP-HA2-based cargo delivery

To assess that the CPP-HA2-mediated protein transduction is applicable in cargo delivery, collagen-fluorescein previously used as a fluorescence-labeled protein cargo in our transdermal study [23] was served as one of examples. A549 cells were treated with collagen-fluorescein alone, R9-HA2-mCherry or R9-HA2-mCherry/collagen-fluorescein complexes and analyzed by confocal microscopy. No green fluorescence could be detected in the cells treated with collagen-fluorescein (Fig. 10). In contrast, the cells treated with R9-HA2-mCherry and R9-HA2-mCherry/collagen-fluorescein complexes in different ratios displayed red and red/green fluorescence, respectively. These results demonstrated

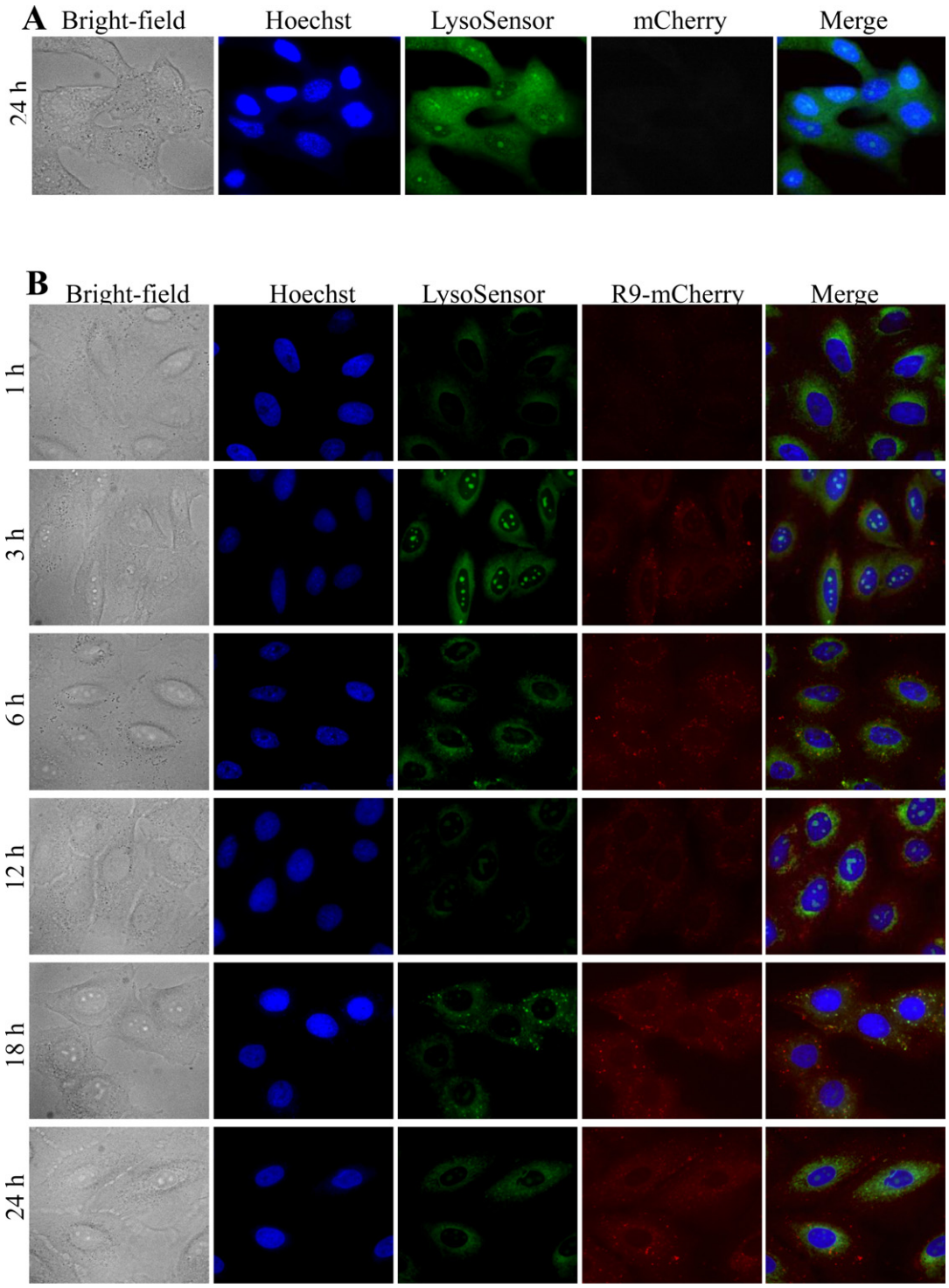

Fig. 7. Subcellular colocalization analysis of CPP-HA2-mediated protein transduction. Cells were treated with 30 μM of mCherry for 24 h (A), or R9-mCherry (B) or R9-HA2-mCherry (C) for 1, 3, 6, 12, 18 and 24 h and then stained with Hoechst 33342 and LysoSensor Green DND-153. Cells were treated with 30 μM of R9-HA2-mCherry for 6 h, R9-mCherry or R9-HA2-NLS-mCherry for 12 h and then stained with Hoechst 33342 and FITC-labeled anti-EEA1 antibody (D). Images were recorded with a BD pathway system at a magnification of 600×. BFP (blue), GFP (green) and RFP (red) channels in the microscope are used to reveal the distribution of nuclei, lysosomes/endosomes and R9-HA2-mCherry, respectively. Overlap between R9-HA2-mCherry (RFP channel) and nuclei (BFP channel) exhibits purple color in merged RFP and BFP images. Overlap between R9-HA2-mCherry (RFP channel) and lysosomes/endosomes (GFP channel) exhibits yellow color in merged RFP and GFP images. (For interpretation of the references to color in this figure legend, the reader is referred to the web version of the article.)

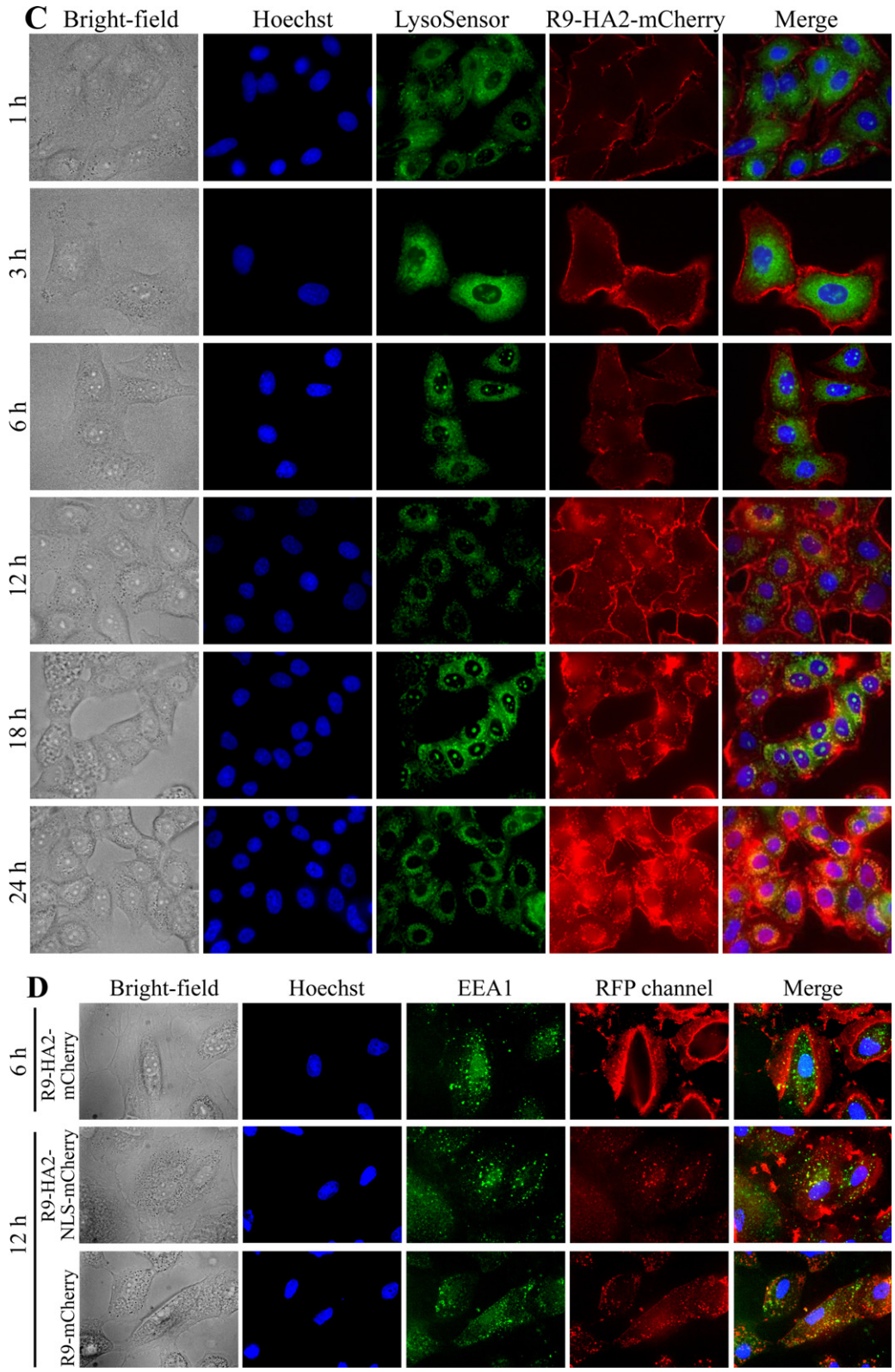

Fig. 7. (*Continued*).

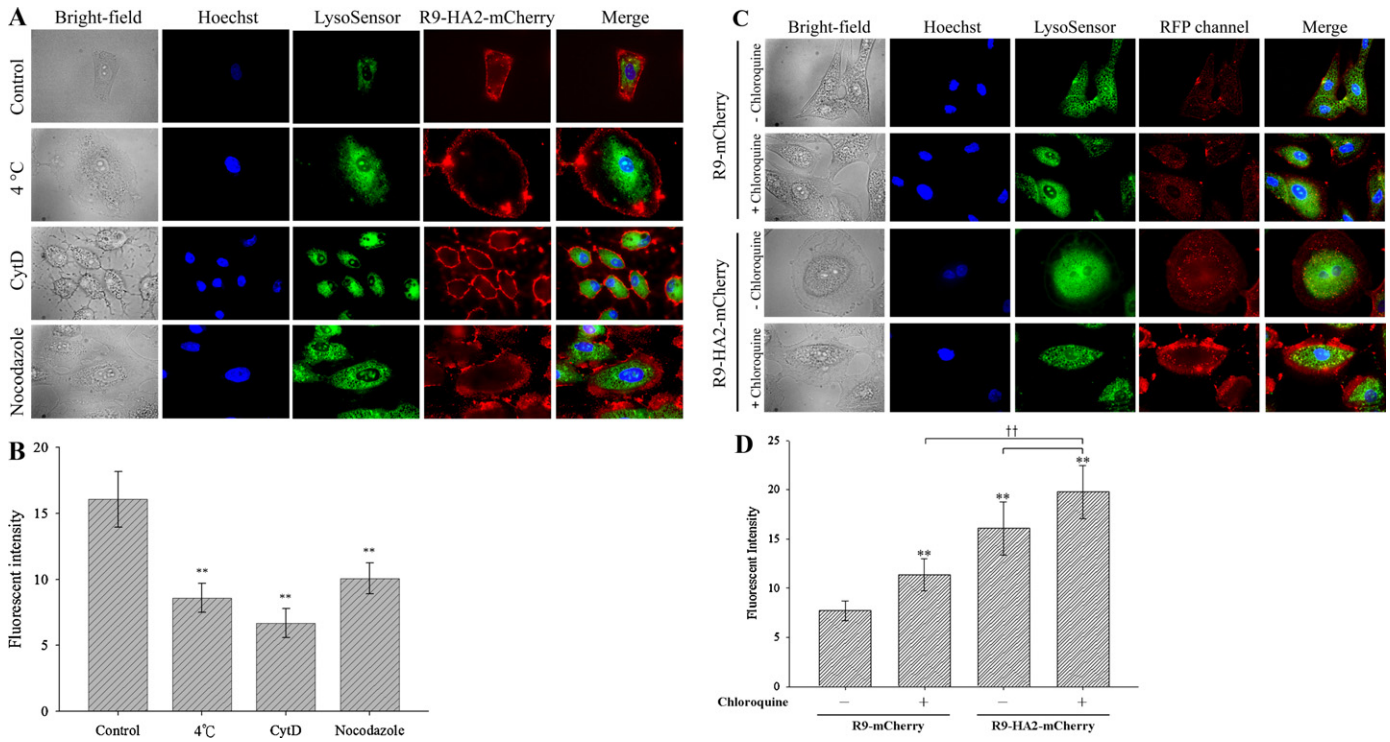

Fig. 8. Effects of endocytic modulators on CPP-HA2-mediated protein transduction. (A) Cells were treated with 30 μM of R9-HA2-mCherry in the absence (control) or presence of low temperature (4 °C), CytD, or nocodazole followed by staining with Hoechst 33342 and LysoSensor Green DND-153 trackers. (B) Data of cells treated with R9-HA2-mCherry in the absence or presence of endocytic inhibitors are presented as mean ± standard deviation from three independent experiments. (C) Cells were treated with R9-mCherry or R9-HA2-mCherry in the absence (−) or presence (+) of chloroquine, followed by staining with Hoechst and LysoSensor trackers. Images were recorded using a BD pathway system at a magnification of 600×. BFP (blue), GFP (green) and RFP (red) channels in the microscope are used to reveal the distribution of nuclei, lysosomes and R9-HA2-mCherry, respectively. (D) Cells were treated with R9-mCherry or R9-HA2-mCherry in the absence or presence of chloroquine. Data are presented as mean ± standard deviation from three independent experiments. Significant differences were set at $P < 0.05$ (*) and $P < 0.01$ (**) between R9-mCherry (control) and others, $P < 0.05$ (†) and $P < 0.01$ (††) between R9-mCherry/chloroquine (control) and R9-HA2-mCherry/chloroquine, or $P < 0.05$ (‡) and $P < 0.01$ (‡‡) between R9-HA2-mCherry (control) and R9-HA2-mCherry/chloroquine. (For interpretation of the references to color in this figure legend, the reader is referred to the web version of the article.)

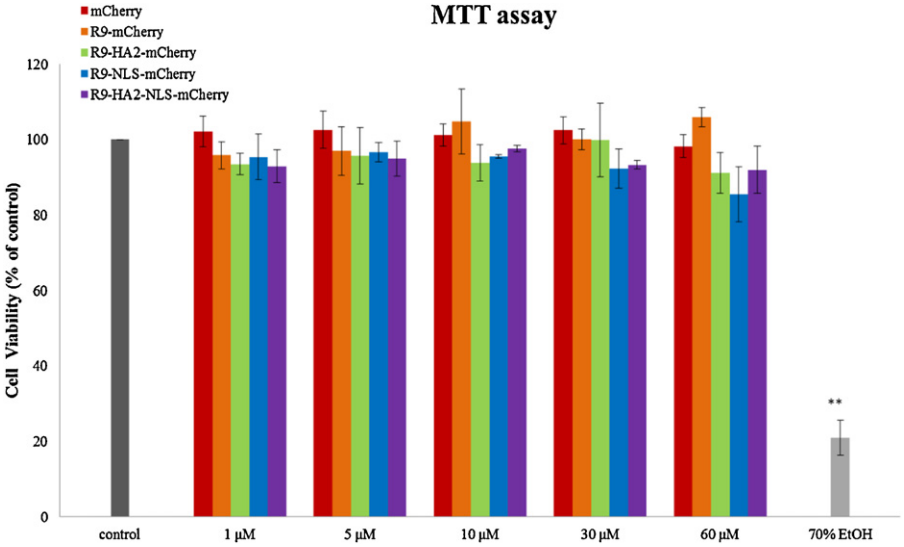

Fig. 9. MTT-based cell viability assay. A549 cells were treated with 1, 5, 10, 30 and 60 μM of mCherry, R9-mCherry, R9-HA2-mCherry, R9-NLS-mCherry or R9-HA2-NLS-mCherry for 24 h. Cells treated with 70% alcohol (EtOH) and PBS (control) served as positive and negative controls, respectively. Cell viability was determined by the ability of the cells to reduce MTT. Data are presented as mean ± standard deviation from three independent experiments. Significant differences were determined at $P < 0.05$ (*) and $P < 0.01$ (**).

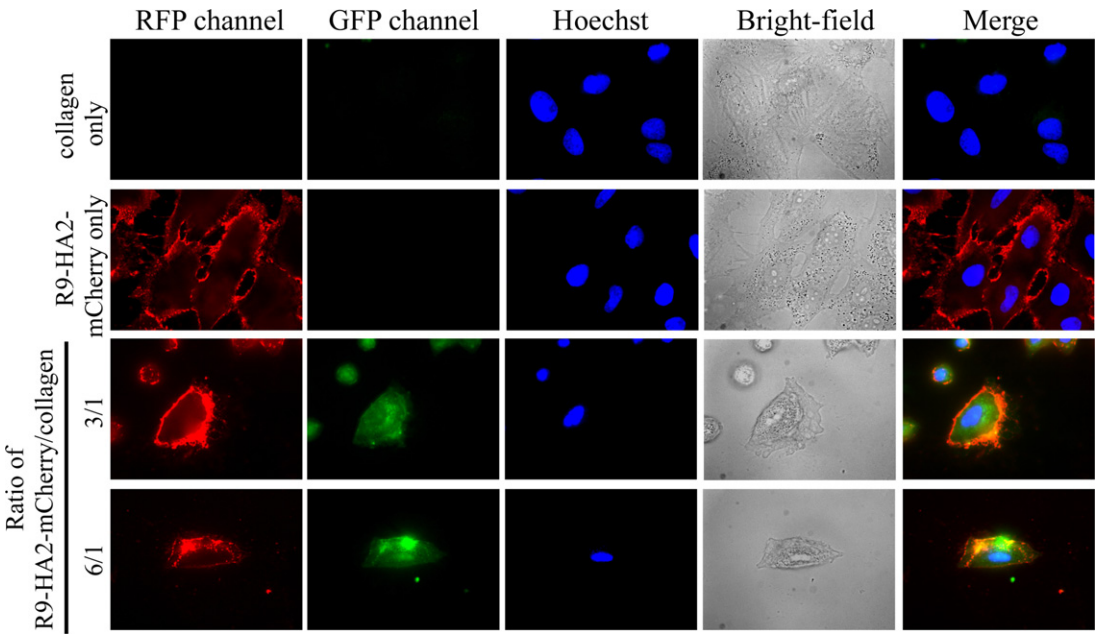

Fig. 10. CPP-HA2-based cargo delivery. A549 cells were treated with collagen-fluorescein alone, R9-HA2-mCherry or R9-HA2-mCherry/collagen-fluorescein complexes in ratios of 3/1 and 6/1. Images were recorded using a BD pathway system at a magnification of 200×. RFP and GFP channels in the microscope are used to reveal the distribution of CPP-HA2 fusion protein and collagen-fluorescein, respectively. Overlap between R9-HA2-mCherry (RFP channel) and collagen-fluorescein (GFP channel) exhibits yellow color in merged RFP and GFP images.

that the CPP-HA2-mediated protein transduction system is indeed applicable in cargo delivery into cells.

4. Discussion

In this report, we demonstrate that the endosomolytic HA2 tag increases cellular uptake, accelerates endosomal escape and promotes even cytosolic distribution of endocytosed CPP-containing RFPs in human A549 cells. We constructed a series of plasmids containing coding sequences of CPP, HA2 and/or NLS fused *RFP*. These plasmids were expressed in bacteria, and the uptake of the purified proteins was measured in A549 cells. Live cell imaging and flow cytometry revealed mechanistic details of cellular uptake and endosomolytic activity. Our results indicate that (1) endocytosis is the major route for cellular uptake of CPP-HA2-tagged RFP, (2) the endosomolytic HA2 peptide promotes the escape of RFPs from endosomes into the cytoplasm and (3) incorporating the HA2 fusion peptide of the CPP-HA2 fusion protein improves cytosolic uptake.

Recent studies indicated that poor intracellular trafficking and limited endosomal release are major factors reducing the efficiency of protein transduction [11,35,43,48,51]. CPP-cargo trapped in endosomes or macropinosomes can be released into the cytosol by membrane perturbation, such as that induced by the INF7 peptide (a glutamic acid-enriched HA2 analog) [13,18,28,36,45,46,61,62]. Contrarily, a recent report showed that the glutamate-rich HA2 analog E5 tags can lyse endosomes, while HA2-protein (E5-TAT-mCherry) conjugates may remain associated with lysed endosomes [30]. In this case, HA2 causes the retention of its fused protein inside endosomes without the diffusion into the cytoplasm even after endosomal lysis takes place [30]. Our results show that R9-HA2-mCherry has the highest protein uptake efficiency among five RFPs examined (Figs. 4–6). Subcellular colocalization and mechanistic studies of CPP-mediated protein internalization indicate that the HA2 tag promotes the escape of RFPs from endosomes into the cytoplasm (Figs. 7 and 8). Together, we conclude that the incorporation of fusogenic HA2 facilitates endosomal disruption and increases cellular internalization of R9-HA2-mCherry.

Studies have used the vacuolating toxin VacA to depict a typical endocytosis timeline. The process requires dynamic F-actin structures on early endosomes for trafficking to late endosomes in HeLa cells [19,20]. The pinocytosis of VacA involves four steps: (1) binding of VacA to the cell by a Rac-dependent process, (2) accumulation of VacA into early endosomes within 10 min in a Cdc42-dependent nonmacropinocytic manner, (3) enrichment of VacA in the early endosomes within 30 min and (4) transfer of VacA from early to late endosomes within 120 min. According to reports on VacA and related compounds [15,19,20,22], our studies of kinetics, molecular mechanisms of uptake and subcellular localization suggest that endosomal disruption caused by HA2 of R9-HA2-mCherry occurs within 0.5–2 h (Figs. 6–8). Our study informed quick endosomal release of R9-HA2-mCherry compared to the other four proteins (Fig. 6). Rapid escape from endosomes may preserve biological activity of delivered cargoes. A report of N-stearylated NLS suggested an enhancement of the CPP-mediated transfection activity by overcoming limitations of cell membrane and nuclear pores [53]. Contrarily, our limited data from the constructs with the NLS tag seemed to suggest a possible interference of the NLS tag with the HA2-enhanced protein transduction at the relatively early time points. The details of this NLS interference remained to be elucidated.

Despite the broad acceptance of CPPs as molecular carriers, the cellular uptake mechanism of CPPs and CPP-cargo is still under vigorous investigation [35,37,43,48]. The internalization of R9-HA2-mCherry was inhibited by incubation at 4 °C and by CytD as well as nocodazole, indicating that the intracellular delivery of R9-HA2-mCherry involves energy-dependent endocytosis (Fig. 8B). Chloroquine, a lysosomotropic agent that prevents endosomal acidification and the degradation by lysosomal enzymes, is often used to improve the efficiency of the gene delivery in laboratory studies [37,60]. The combination of chloroquine and INF7-SGSC peptide caused a synergistic increase of polylysine-mediated DNA

transfection activity in human embryonic kidney (HEK) 293 cells [57]. Our data indicate that chloroquine increases the cellular uptake of R9-HA2-mCherry (Fig. 8C and D) in a non-synergistic manner.

CPPs are very attractive, noncytotoxic candidates for affecting the delivery of therapeutic macromolecules, such as proteins and nucleic acids [12,42,48,51]. The safety of most CPPs has been confirmed in a detailed metabolic analysis [26]. Our data demonstrate that CPPs do not compromise membrane integrity nor result in cytotoxicity of A549 cells as indicated by trypan blue [1,2,4,8,23,54,55], MTT [5,23,55], MTS [59] and sulforhodamine B (SRB) [24,27,32,33] assays. Previous studies used CPPs at 0.1 μM for 2 h [36], 1–20 μM for 3–24 h [28,62], 20–50 μM for 1–2 h [38] or 0–100 μM for 6–24 h [45,46] for fusion protein treatment. Further, the usages of CPP concentrations at or less than 100 μM did not cause cytotoxicity [25]. Together, these findings suggest the HA2 fusion peptide as an effective and safe trigger to enhance protein transduction activity. However, the HA2 fusion peptide located at the N-terminus of CPP-fusion proteins has been reported to be cytotoxic [28,38,45,62]. HA2-TAT [45,62], E5-TAT [28] (5 μM) and N-E5L [38] (100 μM) caused cytotoxicity, while HA2-p53-R9 [36] (0.1 μM) and stearylated INF7 [13] did not. Further, chemically synthesized HA2-R9 peptide with HA2 at the N-terminus exerted a certain degree of cytotoxicity at high concentrations in eukaryotes (manuscript in preparation). Due to data limitation, the true effect of HA2 located at either N- or C-terminus of fusion protein remains unknown. It is important to note that the E5-TAT-mCherry construct was successfully expressed in *E. coli* by blocking the N-terminus of the fusion protein with a cleavable SUMO (small ubiquitin-related modifier) tag [30]. This SUMO tag can be removed by the SUMO protease to obtain an N-terminal glycine residue of the E5 sequence after purification of E5-TAT-mCherry protein. We therefore conjectured that protein with HA2 tagged at the extreme N-terminus may be membrane-lytic or membrane-active [36,52]. It is possible that strong lytic (including endosomolytic) activities of HA2 have been reduced by addition of tags to the N-terminus of HA2. This is a big advantage of our CPP-HA2-tagged proteins with increased plasma membrane association and possibly greater endocytic uptake, because other HA2-fusion proteins have shown much higher toxicity [28,38,45,62].

In order to ascertain whether RFP-fusion proteins cause cytotoxicity during protein transduction, we performed the MTT toxicity test in human A549 cells (Fig. 9). None to very minimal cytotoxicity was observed with any of the five RFPs at concentrations up to 30 μM. When collagen-fluorescein was used as a cargo, our results demonstrated that the CPP-HA2-mediated protein transduction system is applicable in cargo delivery into cells (Fig. 10). These results suggest that CPP tagged with a HA2 fusion peptide at the C-terminus is a relatively safe design for protein transduction promoting agents.

5. Conclusion

Endocytosis is the major route for cellular uptake of CPP-HA2-tagged RFP. The fusogenic HA2 tag facilitates the release of endocytosed RFPs from endosomes into the cytoplasm resulting in a diffuse cytosolic distribution. Remarkably, incorporating the HA2 fusion peptide of the CPP-HA2 fusion protein improved cytosolic uptake without causing cytotoxicity. R9-HA2-mCherry was capable of delivering collagen-fluorescein into cells. Collectively, these results indicate that the CPP-HA2 tag could be an efficient and safe carrier of biologically active molecules.

Acknowledgements

We thank Dr. Roger Y. Tsien for provision of the mCherry plasmid. We are grateful to Dr. Robert S. Aronstam (Missouri University of Science and Technology, USA) for editing the manuscript. This work was supported by Award Number R15EB009530 from the National Institutes of Health (Y.-W.H.), Postdoctoral Fellowship NSC 101-2811-B-259-001 (B.R.L.) and Grant Number NSC 101-2320-B-259-002-MY3 from the National Science Council of Taiwan (H.-J.L.).

References

[1] Chang M, Chou JC, Lee HJ. Cellular internalization of fluorescent proteins via arginine-rich intracellular delivery peptide in plant cells. Plant Cell Physiol 2005;46:482–8.
[2] Chang M, Chou JC, Chen CP, Liu BR, Lee HJ. Noncovalent protein transduction in plant cells by macropinocytosis. New Phytol 2007;174:46–56.
[3] Chang M, Hsu HY, Lee HJ. Dye-free protein molecular weight markers. Electrophoresis 2005;26:3062–8.
[4] Chen CP, Chou JC, Liu BR, Chang M, Lee HJ. Transfection and expression of plasmid DNA in plant cells by an arginine-rich intracellular delivery peptide without protoplast preparation. FEBS Lett 2007;581:1891–7.
[5] Chen YJ, Liu BR, Dai YH, Lee CY, Chan MH, Chen HH, et al. A gene delivery system for insect cells mediated by arginine-rich cell-penetrating peptides. Gene 2012;493:201–10.
[6] Conner SD, Schmid SL. Regulated portals of entry into the cell. Nature 2003;422:37–44.
[7] Cross KJ, Langley WA, Russell RJ, Skehel JJ, Steinhauer DA. Composition and functions of the influenza fusion peptide. Protein Pept Lett 2009;16:766–78.
[8] Dai YH, Liu BR, Chiang HJ, Lee HJ. Gene transport and expression by arginine-rich cell-penetrating peptides in *Paramecium*. Gene 2011;489:89–97.
[9] Deshayes S, Konate K, Aldrian G, Crombez L, Heitz F, Divita G. Structural polymorphism of non-covalent peptide-based delivery systems: highway to cellular uptake. Biochim Biophs Acta 2010;1798:2304–14.
[10] Ding Q, Zhao L, Guo H, Zhang AC. The nucleocytoplasmic transport of viral proteins. Virol Sin 2010;25:79–85.
[11] Edenhofer F. Protein transduction revisited: novel insights into the mechanism underlying intracellular delivery of proteins. Curr Pharm Des 2008;14:3628–36.
[12] El-Sayed A, Futaki S, Harashima H. Delivery of macromolecules using arginine-rich cell-penetrating peptides: ways to overcome endosomal entrapment. AAPS J 2009;11:13–22.
[13] El-Sayed A, Masuda T, Khalil I, Akita H, Harashima H. Enhanced gene expression by a novel stearylated INF7 peptide derivative through fusion independent endosomal escape. J Control Release 2009;138:160–7.
[14] Esbjorner EK, Oglecka K, Lincoln P, Graslund A, Norden B. Membrane binding of pH-sensitive influenza fusion peptides. Positioning, configuration, and induced leakage in a lipid vesicle model. Biochemistry 2007;46:13490–504.
[15] Fischer R, Kohler K, Fotin-Mleezek M, Brock R. A stepwise dissection of the intracellular fate of cationic cell-penetrating peptides. J Biol Chem 2004;279:12625–35.
[16] Frankel AD, Pabo CO. Cellular uptake of the Tat protein from human immunodeficiency virus. Cell 1988;55:1189–93.
[17] Futaki S. Arginine-rich peptides: potential for intracellular delivery of macromolecules and the mystery of the translocation mechanisms. Int J Pharm 2002;245:1–7.
[18] Gao S, Simon MJ, Morrison 3rd B, Banta S. A plasmid display platform for the selection of peptides exhibiting a functional cell-penetrating phenotype. Biotechnol Prog 2010;26:1796–800.
[19] Gauthier NC, Monzo P, Gonzalez T, Doye A, Oldani A, Gounon P, et al. Early endosomes associated with dynamic F-actin structures are required for late trafficking of *H. pylori* VacA toxin. J Cell Biol 2007;177:343–54.
[20] Gauthier NC, Monzo P, Kaddai V, Doye A, Ricci V, Boquet P. Helicobacter pylori VacA cytotoxin: a probe for a clathrin-independent and Cdc42-dependent pinocytic pathway routed to late endosomes. Mol Biol Cell 2005;16:4852–66.
[21] Green M, Loewenstein PM. Autonomous functional domains of chemically synthesized human immunodeficiency virus Tat *trans*-activator protein. Cell 1988;55:1179–88.
[22] Gruenberg J. The endocytic pathways: a mosaic of domains. Nat Rev Mol Cell Biol 2001;2:721–30.
[23] Hou YW, Chan MH, Hsu HR, Liu BR, Chen CP, Chen HH, et al. Transdermal delivery of proteins mediated by non-covalently associated arginine-rich intracellular delivery peptides. Exp Dermatol 2007;16:999–1006.
[24] Hu JW, Liu BR, Wu CY, Lu SW, Lee HJ. Protein transport in human cells mediated by covalently and noncovalently conjugated arginine-rich intracellular delivery peptides. Peptides 2009;30:1669–78.
[25] Jones SW, Christison R, Bundell K, Voyce CJ, Brockbank SM, Newham P, et al. Characterisation of cell-penetrating peptide-mediated peptide delivery. Br J Pharmacol 2005;145:1093–102.
[26] Kilk K, Mahlapuu R, Soomets U, Langel U. Analysis of in vitro toxicity of five cell-penetrating peptides by metabolic profiling. Toxicology 2009;265:87–95.

[27] Lee CY, Li JF, Liou JS, Charng YC, Huang YW, Lee HJ. A gene delivery system for human cells mediated by both a cell-penetrating peptide and a *piggyBac* transposase. Biomaterials 2011;32:6264–76.
[28] Lee YJ, Erazo-Oliveras A, Pellois JP. Delivery of macromolecules into live cells by simple coincubation with a peptide. ChemBioChem 2010;11:325–35.
[29] Lee YJ, Johnson G, Pellois JP. Modeling of the endosomolytic activity of HA2-TAT peptides with red blood cells and ghosts. Biochemistry 2010;49:7854–66.
[30] Lee YJ, Johnson G, Peltier GC, Pellois JP. A HA2-fusion tag limits the endosomal release of its protein cargo despite causing endosomal lysis. Biochim Biophs Acta 2011;1810:752–8.
[31] Liu BR, Huang YW, Chiang HJ, Lee HJ. Cell-penetrating peptide-functionized quantum dots for intracellular delivery. J Nanosci Nanotechnol 2010;10:7897–905.
[32] Liu BR, Huang YW, Winiarz JG, Chiang HJ, Lee HJ. Intracellular delivery of quantum dots mediated by a histidine- and arginine-rich HR9 cell-penetrating peptide through the direct membrane translocation mechanism. Biomaterials 2011;32:3520–37.
[33] Liu BR, Li JF, Lu SW, Lee HJ, Huang YW, Shannon KB, et al. Cellular internalization of quantum dots noncovalently conjugated with arginine-rich cell-penetrating peptides. J Nanosci Nanotechnol 2010;10:6534–43.
[34] Lu SW, Hu JW, Liu BR, Lee CY, Li JF, Chou JC, et al. Arginine-rich intracellular delivery peptides synchronously deliver covalently and noncovalently linked proteins into plant cells. J Agricult Food Chem 2010;58:2288–94.
[35] Madani F, Lindberg S, Langel U, Futaki S, Graslund A. Mechanisms of cellular uptake of cell-penetrating peptides. J Biophys 2011;2011:414729.
[36] Michiue H, Tomizawa K, Wei FY, Matsushita M, Lu YF, Ichikawa T, et al. The NH2 terminus of influenza virus hemagglutinin-2 subunit peptides enhances the antitumor potency of polyarginine-mediated p53 protein transduction. J Biol Chem 2005;280:8285–9.
[37] Nakase I, Kobayashi S, Futaki S. Endosome-disruptive peptides for improving cytosolic delivery of bioactive macromolecules. Biopolymers 2010;94:763–70.
[38] Neundorf I, Rennert R, Hoyer J, Schramm F, Lobner K, Kitanovic I, et al. Fusion of a short HA2-derived peptide sequence to cell-penetrating peptides improves cytosolic uptake, but enhances cytotoxic activity. Pharmaceuticals 2009;2:49–65.
[39] Noguchi H, Matsushita M, Kobayashi N, Levy MF, Matsumoto S. Recent advances in protein transduction technology. Cell Transplant 2010;19:649–54.
[40] Plank C, Oberhauser B, Mechtler K, Koch C, Wagner E. The influence of endosome-disruptive peptides on gene transfer using synthetic virus-like gene transfer systems. J Biol Chem 1994;269:12918–24.
[41] Pooga M, Hallbrink M, Zorko M, Langel U. Cell penetration by transportan. FASEB J 1998;12:67–77.
[42] Raagel H, Saalik P, Pooga M. Peptide-mediated protein delivery – which pathways are penetrable? Biochim Biophys Acta 2010;1798:2240–8.
[43] Schmidt N, Mishra A, Lai GH, Wong GC. Arginine-rich cell-penetrating peptides. FEBS Lett 2010;584:1806–13.
[44] Shaner NC, Campbell RE, Steinbach PA, Giepmans BNG, Palmer AE, Tsien RY. Improved monomeric red, orange and yellow fluorescent proteins derived from *Discosoma* sp. red fluorescent protein. Nat Biotechnol 2004;22:1567–72.
[45] Sugita T, Yoshikawa T, Mukai Y, Yamanada N, Imai S, Nagano K, et al. Improved cytosolic translocation and tumor-killing activity of Tat-shepherdin conjugates mediated by co-treatment with Tat-fused endosome-disruptive HA2 peptide. Biochem Biophys Res Commun 2007;363:1027–32.
[46] Sugita T, Yoshikawa T, Mukai Y, Yamanada N, Imai S, Nagano K, et al. Comparative study on transduction and toxicity of protein transduction domains. Br J Pharmacol 2008;153:1143–52.
[47] Terpe K. Overview of tag protein fusions: from molecular and biochemical fundamentals to commercial systems. Appl Microbiol Biotechnol 2003;60:523–33.
[48] van den Berg A, Dowdy SF. Protein transduction domain delivery of therapeutic macromolecules. Curr Opin Biotechnol 2011;22:888–93.
[49] Vives E, Brodin P, Lebleu B. A truncated HIV-1 Tat protein basic domain rapidly translocates through the plasma membrane and accumulates in the cell nucleus. J Biol Chem 1997;272:16010–7.
[50] Wadia JS, Dowdy SF. Protein transduction technology. Curr Opin Biotechnol 2002;13:52–6.
[51] Wadia JS, Stan RV, Dowdy SF. Transducible TAT-HA fusogenic peptide enhances escape of TAT-fusion proteins after lipid raft macropinocytosis. Nat Med 2004;10:310–5.
[52] Wagner E. Application of membrane-active peptides for nonviral gene delivery. Adv Drug Deliv Rev 1999;38:279–89.
[53] Wang HY, Chen JX, Sun YX, Deng JZ, Li C, Zhang XZ, et al. Construction of cell penetrating peptide vectors with N-terminal stearylated nuclear localization signal for target delivery of DNA into the cell nuclei. J Control Release 2011;155:26–33.
[54] Wang YH, Chen CP, Chan MH, Chang M, Hou YW, Chen HH, et al. Arginine-rich intracellular delivery peptides noncovalently transport protein into living cells. Biochem Biophys Res Commun 2006;346:758–67.
[55] Wang YH, Hou YW, Lee HJ. An intracellular delivery method for siRNA by an arginine-rich peptide. J Biochem Biophys Methods 2007;70:579–86.
[56] Wharton SA, Martin SR, Buigrok RWH, Skehel JJ, Wiley DC. Membrane fusion by peptide analogues of influenza virus haemagglutinin. J Gen Virol 1988;69:1847–57.
[57] Wolfert MA, Seymour LW. Chloroquine and amphipathic peptide helices show synergistic transfection in vitro. Gene Ther 1998;5:409–14.
[58] Xie Y, Gong J, Li M, Fang H, Xu W. The medicinal potential of influenza virus surface proteins: hemagglutinin and neuraminidase. Curr Med Chem 2011;18:1050–66.
[59] Xu Y, Liu BR, Chiang HJ, Lee HJ, Shannon KB, Winiarz JG, et al. Nona-arginine facilitates delivery of quantum dots into cells via multiple pathways. J Biomed Biotechnol 2010;2010:948543.
[60] Yang S, Coles DJ, Esposito A, Mitchell DJ, Toth I, Minchin RF. Cellular uptake of self-assembled cationic peptide-DNA complexes: multifunctional role of the enhancer chloroquine. J Control Release 2009;135:159–65.
[61] Ye SF, Tian MM, Wang TX, Ren L, Wang D, Shen LH, et al. Synergistic effects of cell-penetrating peptide Tat and fusogenic peptide HA2-enhanced cellular internalization and gene transduction of organosilica nanoparticles. Nanomedicine 2012;8:833–41.
[62] Yoshikawa T, Sugita T, Mukai Y, Yamanada N, Nagano K, Nabeshi H, et al. Organelle-targeted delivery of biological macromolecules using the protein transduction domain: potential applications for peptide aptamer delivery into the nucleus. J Mol Biol 2008;380:777–82.